Electrical transport and magnetotransport studies in WEAK ITINERANT amorphous $Fe_{90-x}Mn_xZr_{10}$ $(0 \leqslant x \leqslant 16)$ alloys

V. Srinivas* and A. Perumal†
Department of Physics, Indian Institute of Technology, Kharagpur-721302, India

A. K. Nigam and G. Chandra
Low Temperature Physics, Tata Institute of Fundamental Research, Bombay, India

A. E. George and R. A. Dunlap
Department of Physics, Dalhousie University, Halifax, Nova Scotia, Canada B3H 3J5
(Received 19 March 2003; published 23 September 2003)

Zero-field and in field electrical resistivity, magnetoresistivity, and magnetization measurements have been performed in the temperature range of 4.2 K to 300 K and in the fields up to 60 kOe on amorphous $Fe_{90-x}Mn_xZr_{10}$ $(0 \leqslant x \leqslant 16)$ alloys. Unusual properties such as a broad resistivity minimum in the higher-temperature region and a resistivity minimum close to Curie temperature were observed for alloys with a certain Mn content. An analysis of the resistivity data using existing theories reveals the actual functional dependencies of resistivity on temperature in different temperature ranges. The enhancement of spin fluctuation with Mn concentration has been observed from resistivity data and is further supported by the magnetization data. A comparative study of magnetic and transport properties indicates that remarkable effects due to magnetic ordering are present in both resistivity and magnetoresistivity. The observed composition dependence of the spontaneous resistive anisotropy is explained in terms of the two-current-conduction model. The determined values of composition dependence of spin-up and spin-down residual resistivity provide conclusive evidence of weak itinerant ferromagnetism over the entire composition range of the present investigation. These results are further supported by the high-field dc susceptibility data obtained from magnetization measurements.

DOI: 10.1103/PhysRevB.68.104425 PACS number(s): 75.30.Kz, 75.40.Cx, 75.50.Kj, 75.50.Lk

I. INTRODUCTION

Magnetism in amorphous transition-metal (TM) alloys has been extensively investigated from both fundamental and technological points of view. In particular, randomly diluted magnetic systems with short-range interactions have captured the attention of scientists in recent years.[1,2] The random addition of antiferromagnetic (AFM) exchange interactions in a ferromagnetic (FM) Heisenberg spin system leads to a loss of FM order through the effects of exchange frustration. In the ultimate case, a spin glass (SG) is formed with random isotropic spin freezing with neither net magnetization nor long-range FM order. At lower levels of exchange frustration, the system displays characteristics of both extremes as long-range FM order coexists with SG order. On warming such a system from low temperature the SG order first melts at a temperature (T_{sg}) followed by the loss of FM order at the Curie temperature (T_c). Although such behavior has been observed in a number of systems, the amorphous alloys are found to be the most suitable for the systematic study of these phenomena.

Amorphous (a-) $Fe_{90}Zr_{10}$, for example, shows a double transition (reentrant) behavior below room temperature, i.e., as the temperature is lowered a transition from paramagnetic to FM order occurs at about 230 K (T_c) and on further cooling another transition from FM to the SG regime occurs at about 35 K (T_{sg}). There have been extensive studies on a-FeZr and related systems to understand the magnetic structure of these alloys.[3–11] On the theoretical front, calculations have been done on alloys near the percolation threshold and have suggested that FM order coexists with SG ordering in these limits.[12] Since the reentrant SG behavior is connected with a rearrangement of the spin structure at low temperatures, it is expected that the existence of the reentrant phenomenon may lead to an unusual magnetic contribution to the electrical resistivity. In fact, the observed broad minimum in resistivity at a temperature (T_{min}) is close to T_c and this indicates a correlation between magnetic and electrical transport properties.[5,9,13] Therefore, it is important to investigate whether the magnetic properties of these alloys are correlated to electrical transport, particularly near the magnetic phase transitions. There have been some attempts to understand the various contributions to the resistivity by studying the effects of pressure,[3] magnetic field,[6] and temperature,[7] and by analyzing the temperature dependence of resistivity data using different models.[5,14,15]

The low-temperature galvanomagnetic properties of amorphous alloys and nanocrystals dispersed in an amorphous matrix have become a subject of renewed interest[16–18] due to the observation of giant magnetoresistance in some mixed interaction systems. The presence of structural disorder gives rise to two major effects:

(i) An increase in the localization of the electron wave function. If the disorder is sufficient, a transition occurs from the metallic to the insulating state. Weak localization occurs if the disorder is not sufficient to give rise to the completely

localized states, but is high enough to influence the transport properties.

(ii) Diffusive motion of the electrons.

Since both of these mechanisms are directly affected by the magnetic field, new contributions to the magnetoresistivity are expected in such alloys. The magnetoresistance (MR) of magnetic alloys is predicted to be sensitive only to changes in the magnetic correlation on a scale of the order of the electron mean free path, whereas the magnetization depends on both the short- and the long-range FM orders as well as on the rotation of the FM domains as a response to the applied field. Therefore, the study of MR not only provides a unique way to obtain several important and fundamental parameters that are related to the electron-transport properties, but also provides complementary information about the microscopic magnetization and can aid in understanding the relationship between magnetic interactions and electron-scattering mechanisms.

Another interesting area of research is the thermal critical behavior of the partially frustrated systems near the magnetic order-disorder phase transition. Careful analysis of the data from various magnetic measurements have, in some cases, yielded values of the critical exponents β and γ larger[19,20] than those theoretically predicted for the ordered three-dimensional (3D) nearest-neighbor isotropic Heisenberg ferromagnet, while in other cases these values are in agreement with the 3D Heisenberg model. Substantially diverse results for critical exponents for these materials continue to appear in the literature. In general, the exponents are obtained from ac susceptibility and/or dc magnetization measurements. In some systems, where magnetic and transport data are interrelated the exponents can be evaluated and verified by independent methods. Although there are some reports on electrical transport behavior of binary FeZr amorphous alloys, there is no clear consensus as to whether there is any interrelation between the magnetic and electrical properties. For example, Plaza *et al.*[7] suggested that the resistivity behavior was dominated by structural, rather than magnetic, effects. On the other hand, transport studies under pressure and applied magnetic field suggest a significant spin-dependent contribution to the resistivity. Recently Suzuki *et al.*[18] attributed the spin-dependent scattering to the destruction of FM order (due to increase in AFM interactions) in FeZrCuRu alloys.

In the a-$Fe_{100-c}Zr_c$($7<c<12$) system, rapid changes in magnetic character occur over a narrow range of compositions and the reentrant SG behavior vanishes at about 6-at. % Zr, making investigations on melt spun samples rather difficult. Replacement of Fe by many other TM or metalloid elements destroys reentrant SG behavior. It has been found that substitution of Mn for Fe decreases T_c almost linearly and the reentrant behavior is preserved up to $x=16$ in the amorphous phase.[21] Therefore, Mn-substituted samples are most suited to investigate the development of the reentrant SG behavior and its consequences on transport over a large concentration range. Magnetic[4,8,11] and electrical transport[6] studies have been reported on Mn-substituted a-FeZr alloys. However, these studies do not address the questions concerning the interrelationship between magnetic and electrical transport properties. In the present paper, we report the zero-field and in field electrical resistivity measurements, magnetoresistivity measurements, and the magnetic behavior of amorphous $Fe_{90-x}Mn_xZr_{10}$ ($x=0$–16) alloys in the temperature range of 4.2 K to 300 K. From these measurements, we have attempted to obtain complementary information on electrical transport and to investigate whether or not the magnetic properties of these alloys are correlated to electron-scattering mechanisms. Particular emphasis is placed on the regions near magnetic phase transitions with an idea to improve our understanding of the effects of magnetic interactions on the electron-scattering mechanisms.

II. EXPERIMENTAL METHODS

Amorphous $Fe_{90-x}Mn_xZr_{10}$ ($x=0$ to 16) alloy ribbons were prepared by arc melting high-purity elemental components followed by quenching from the melt onto a single copper roller in an argon atmosphere. The amorphous nature of the samples was confirmed by x-ray diffraction using Cu-K_α radiation and by scanning electron microscope studies. The resistivity measurements under zero field and in field were performed at a constant current of 10 mA in applied fields of up to 40 kOe over the temperature range of 4.2 K to 300 K, employing the standard four-probe-dc method. Considerable care was taken to ensure that the current-voltage contacts were collinear so that no Hall voltage component contributed to the magnetoresistive anisotropy. The magnetoresistance measurements were performed over the field range 0 to 40 kOe at various temperatures in both longitudinal and transverse geometries. The temperature for in field measurements was monitored with a calibrated Lakeshore carbon-glass sensor while a Lakeshore silicon-diode sensor was used for zero-field measurements. The magnetic characterization[21] of the samples were done by low-field ac susceptibility (ACS) measurements and high-field dc magnetization measurements, performed in the field range 0 to 60 kOe and for temperatures from 4.2 K to 300 K.

III. RESULTS AND DISCUSSION

A. Temperature dependence of resistivity

The temperature dependence of the normalized electrical resistivity $[r(T)=\rho(T)/\rho(4.2\ \mathrm{K})]$ for a-$Fe_{90-x}Mn_xZr_{10}$ ($x=0$, 4, and 8) samples is shown in Fig. 1. This method of presenting the data helps to eliminate uncertainty in the measurement of sample dimensions, especially thickness of the sample. A comparison of magnetic and transport parameters obtained from ACS and electrical resistivity measurements, respectively, are summarized in Table I. The following important observations can be made from the results presented in Fig. 1 and Table I:

(i) The change in $r(T)$ is about 3% for $x=0$ and 1% for $x=8$.

(ii) The resistivity decreases continuously with decreasing temperature from 300 K to T_{min} and increases with further decreasing temperature. For all samples the variation of resistivity is characterized by a resistivity minimum close to the magnetic ordering temperature (indicated by the arrow in Fig. 1).

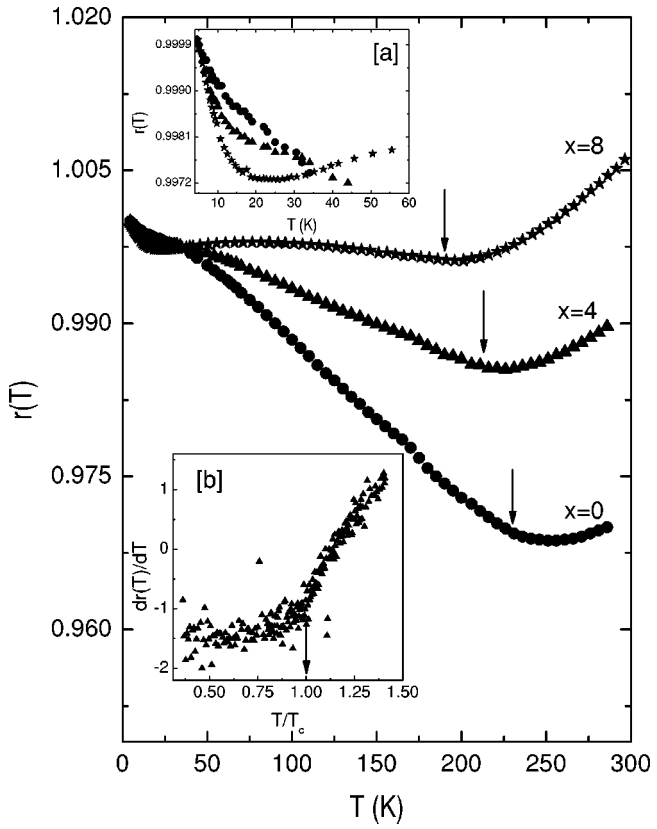

FIG. 1. Normalized resistivity, $r(T)$, as a function of temperature for amorphous $Fe_{90-x}Mn_xZr_{10}$ ($x=0$, 4, and 8); Inset: (a) Enlarged portion of low-temperature region. (b) The temperature derivative of resistivity is plotted against reduced temperature with respect to the Curie temperature for the $Fe_{86}Mn_4Zr_{10}$ alloy.

(iii) T_{min} decreases with increasing Mn concentration.

(iv) For $x=0$ and 4, a small anomaly in the $r(T)$ curve at low temperature is observed whereas for $x=8$ a clear second minimum (T_{ml}) is observed at low temperature (see Fig. 1(a)). Although there is no obvious discontinuity in the resistivity curve near T_c, the temperature derivative of resistivity (Fig. 1(b)) shows an distinct anomaly at a temperature close to T_c indicating the existence of a phase transition.[3]

As shown in Table I, both T_c and T_{min} decrease monotonically with a rate of 5.3 K and 7 K per at. % of Mn, respectively. These observations are similar to those for binary FeZr alloys[9] and suggest that the resistivity minimum around T_c is closely correlated to the magnetic behavior. Such behavior is further supported by pressure-dependent studies of *a*-FeZr alloys.[3,17] Low-field magnetization data show that the substitution of Mn atoms in place of Fe increases the magnetic disorder.[4,8,11]

TABLE I. Magnetic and electrical resistivity parameters for amorphous $Fe_{90-x}Mn_xZr_{10}$ alloys; T_{sg} (spin-glass freezing temperature), T_c (Curie temperature), T_{min} (temperature at which minimum appears in resistivity curve), T_{ml} (low-temperature minimum in the resistivity curve), and ρ(5 K) and ρ(300 K) (resistivities at 5 K and 300 K, respectively). $\Delta r=[\rho(\max)-\rho(\min)]/\rho(\min)$ (maximum change in the resistivity curve).

x	T_{sg} (K)	T_c (K)	T_{min} (K)	T_{ml} (K)	ρ(5 K) $\mu\Omega$ cm	ρ(300 K) $\mu\Omega$ cm	Δr (%)
0	36	227	251		180	174	3.13
4	46	211	226		194	192	1.45
8	54	185	195	19	213	215	1.11
12	65	154	173		237	236	1.65

In order to further substantiate these results, we have performed temperature-dependent resistivity measurements in applied magnetic fields of 7 kOe and 40 kOe. The temperature dependence of resistivity data taken under different applied external fields is depicted in Fig. 2 for *a*-$Fe_{90-x}Mn_xZr_{10}$ ($x=0$ to 12) alloys. The relevant parameters are listed in Table II. Although the shape of the resistivity curves is not significantly affected by the application of an external magnetic field, a clear suppression of the magnitude of the resistivity minimum is observed (see Table II). Since the observed resistivity minimum is broad for higher Mn substitution, the uncertainty in determining T_{min} is correspondingly large. However, a definite shift in T_{min} is observed on application of an external magnetic field in contrast to the behavior observed in earlier studies on binary alloys.[7] A similar behavior has been observed in other crystalline[22] and amorphous[23] systems with mixed exchange interactions. Both composition dependence and in field resistivity studies suggest the presence of significant magnetic contributions to the resistivity.

Certain features of the resistivity minimum, such as the observation of a nearly logarithmic temperature dependence[24] just below T_{min} and the suppression of the resistivity minimum upon the application of a magnetic field, have similarities with the Kondo effect.[25] However, the Kondo-like scattering model could not describe the existence of a positive MR (Ref. 26) in binary *a*-FeZr alloys. On the other hand, the observed positive MR in other amorphous alloys has been explained using quantum interference effects, i.e., weak localization theory,[27] and also by electron-electron interaction (EEI) theory.[28] The localization phenomenon gives either a negative MR or a positive MR (in case of the presence of strong spin-orbit scattering), while EEI theory shows a positive MR and a $-\sqrt{T}$ dependence of the resistivity at low temperatures. As shown in Fig. 3(a), the low-temperature resistivity data could be fitted to $-\sqrt{T}$ behavior. However, strong deviations can be noticed at higher temperatures.

Spin fluctuations play an important role in thermal variation of magnetization in weak itinerant magnets. These effects can significantly alter the temperature variation of the electrical resistivity[29] in these systems. In fact, in the model proposed by Ueda and Moriya based on Moriya and Kawabata,[30] the effect of spin fluctuations is shown to play an essential role. This theory provides more realistic information on the temperature dependence of the electrical resistivity and the magnetization behavior. Since there is no theory that describes the temperature and field dependence of resistivity over the entire temperature range of the present investigation, we have made an attempt to bring out the exact functional dependence of resistivity as a function of temperature in different temperature ranges so as to identify the

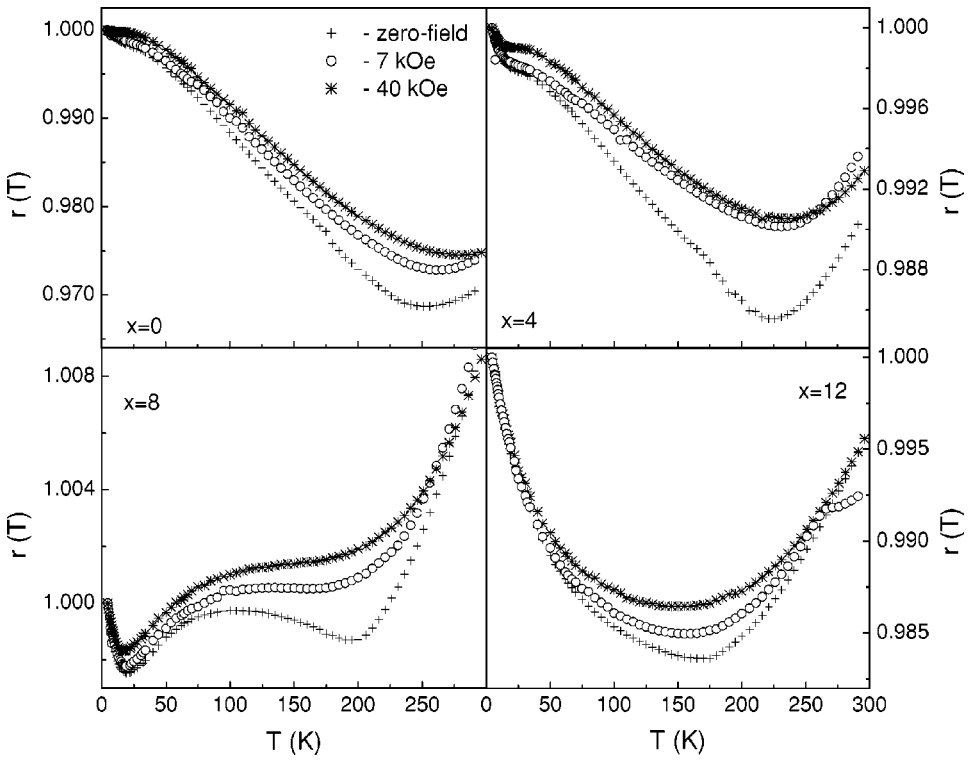

FIG. 2. Normalized resistivity, $r(T)$, as a function of temperature for amorphous $Fe_{90-x}Mn_xZr_{10}$ ($x=0$, 4, 8, and 12) alloys under different applied magnetic fields.

dominant scattering mechanism responsible for $r(T)$ in the specified temperature ranges. Assuming the validity of Matthiessen's rule, the $r(T)$ data for $T>30$ K have been analyzed in terms of following expressions,

$$r(T)=r(0)-aT^{3/2}+bT^2, \tag{1}$$

$$r(T)=r'(0)-a'T^{3/2}+b'T^{5/3}, \tag{2}$$

$$r(T)=r''(0)-a''T+b''T^{5/3}. \tag{3}$$

In the theoretical model proposed by Ueda and Moriya[29] for weak ferromagnets, the various contributions that arise from the scattering of conduction electrons by spin fluctuations (SFs) vary with T as $\rho_{SF}\propto T^2$ for $T\ll T_c$ and $\rho_{SF}\propto T^{5/3}$ for T just above and below T_c. The third term in Eqs. (1)–(3) represents the SF contribution to $r(T)$, while the second term in Eqs. (1)–(3) arises from WL effects. These three expressions provide the best least-squares fits (based on the minimum in χ^2_{fit} values[11] listed in Table II) to the $r(T)$ data in the temperature ranges $0.23T_c<T<0.73T_c$, $0.74T_c<T<0.93T_c$, and $1.05T_c<T<1.29T_c$, respectively. The temperature ranges over which the above expressions clearly describe the $r(T)$ data [Figs. 3(b) and 3(c)] and the optimum values of fitting parameters are given in Table II. A different theoretical treatment[16,31] has predicted the temperature dependence of inelastic scattering time (τ_{ie}) in the form of $\tau_{ie}=AT^{-p}$ (where A is constant) for $T<T_c$ with the value of p varying from 2 to 5 depending on the temperature range and $p=1$ for high temperatures. If we assume the value of p is 3 then the interpretation is consistent with expectations, i.e., the rate of increase of inelastic-scattering time with temperature decreases from T^3 to T^2 as the temperature is in-

TABLE II. Results of the theoretical fits {based on $\chi^2_{fit_i}$ [$i=1$, 2, and 3 for Eqs. (1), (2), and (3), respectively] values} to $r(T)$ data with external field for amorphous $Fe_{90-x}Mn_xZr_{10}$ alloys based on Eqs. (1)–(3).

x	H (kOe)	T_{ml} (K)	T_{min} (K)	Δr (%)	a (10^{-5} K$^{-3/2}$)	b (10^{-5} K^{-2})	$\chi^2_{fit_1}$ (10^{-9})	a' (10^{-4} K$^{-3/2}$)	b' (10^{-5} K$^{-5/3}$)	$\chi^2_{fit_2}$ (10^{-9})	a'' (10^{-4} K^{-1})	b'' (10^{-5} K$^{-5/3}$)	$\chi^2_{fit_3}$ (10^{-9})
	0		251	3.13	2.402	9.689	0.136	1.343	4.667	0.079	9.801	1.439	1.136
0	7		263	2.72	1.180	8.251	0.210	0.310	2.009	0.046	6.349	1.331	2.221
	40		281	2.57	0.573	6.004	0.276	0.139	1.795	0.098	7.321	1.296	1.857
	0		226	1.45	2.402	10.608	0.321	6.532	4.607	1.236	7.112	3.499	0.471
4	7		228	0.99	2.323	08.231	0.613	5.684	4.325	1.649	6.856	3.210	0.967
	40		236	0.95	1.998	06.534	0.463	4.956	4.301	2.892	6.231	3.102	0.740
	0	19.3	195	1.11	5.735	13.208	0.512	9.352	7.861	2.316	9.801	5.596	4.368
8	7	19.8	168	0.91	4.671	11.130	0.451	8.654	7.521	4.786	8.752	4.869	3.462
	40	17.6	151	0.72	3.945	08.121	0.873	8.524	7.231	5.115	8.231	4.201	1.965

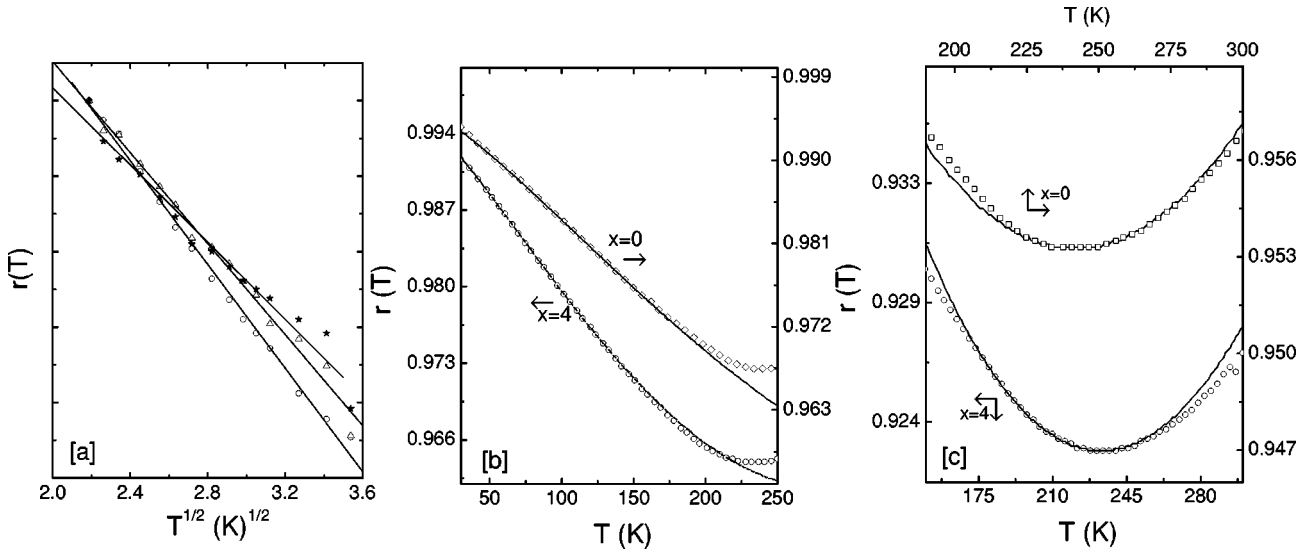

FIG. 3. The normalized resistivity plotted against (a) $\sqrt{T}$ in the low-temperature region (○-0, △-4, and ⋆-8), (b) intermediate region, and (c) close to but above T_c for amorphous $Fe_{90-x}Mn_xZr_{10}$ alloys with $x=0$ and 4. The continuous line passing through the data is the best fit to (a) $\sqrt{T}$, (b) Eq. (1), and (c) Eq. (3).

creased towards the Debye temperature. Therefore, the second term in Eqs. (1)–(3) has its origin in the destruction of phase coherence by the electron-phonon scattering, which, in the present case, is the dominant scattering process at intermediate temperatures. In order to bring actual physical meaning to Eqs. (2) and (3), we have compared all the parameters. From this comparison, we conclude that the second term in Eqs. (2) and (3) is mainly responsible for the dephasing mechanism, while the third term indicates the dominant contribution of SF to the resistivity. Moreover the increase in magnitude of b' and b'' might be due to an enhancement of SF by Mn substitution. Similar behavior was observed in our previous magnetic measurements.[10] The important parameters of interest obtained from magnetic[32] and electrical resistivity measurements are compared in Fig. 4, where similar and systematic trends were observed for both magnetic field and concentration.

B. Magnetoresistance

In order to further investigate the magnetic contribution to resistivity, the field, temperature, and composition dependence of the MR have been studied as discussed in the sections below.

1. Field dependence of magnetoresistance

Figure 5 shows the longitudinal MR (LMR) and transverse MR (TMR) as a function of applied field (H) for all the samples at selected temperatures: $T<T_{sg}$, $T_{sg}<T<T_c$, and $T>T_c$. The MR calculated in the present investigation is defined as $(\Delta\rho/\rho)_{(\perp)(||)}=\{[\rho(H,T)-\rho(0,T)]/\rho(0,T)\}_{(\perp)(||)}$, where $\rho(H,T)$ is the resistance of the sample under the magnetic field at a particular temperature and $\perp(||)$ indicates the field applied in the transverse (longitudinal) direction. In all cases, it is seen that LMR is positive (solid circles in Fig. 5) and decreases with increasing Mn concentration. This reduction in MR could be attributed to the formation of zero-field regions in the sample due to an increase in antiferromagnetically coupled spins. In fact, the effect of competing interactions could be clearly observed in the form of a zero-field tail in a hyperfine field distribution by means of Mössbauer studies.[33] The observed MR is smaller in the SG region than in the FM region and above T_c it becomes progressively smaller and takes on an approximate H^2 dependence. The composition dependence of the spontaneous magnetization and spontaneous LMR show similar behavior (see Fig. 6). This also suggests that the magnetic and electrical properties are interrelated in these random magnets. On the other hand, the TMR is negative (open circles in Fig. 5) at low field and crosses over to positive values at higher fields resulting in a minimum in MR. The magnitude of TMR changes with Mn concentration and shows different trends at high and low temperatures, while LMR shows a consistent increase with field at all temperatures. The steep decrease (increase) of TMR (LMR) seems to be related to the FM character of the sample as it disappears above the Curie temperature. In order to further investigate the MR behavior in the critical region the temperature dependence of the MR has been studied and is discussed below.

2. Temperature dependence of the magnetoresistance

The temperature variation of $\Delta\rho/\rho$ for the reentrant SG alloys ($x=0$, 4, 8, and 12) from 4.2 K to 300 K and in fields of 7 kOe and 40 kOe is shown in Fig. 7. The temperature dependence of the MR seems to be similar for all concentrations. Some of the salient features are as follows:

(i) Low-field MR curves at low temperatures show large negative values of the MR and these cross over to positive values close to T_c, while the high-field MR shows this crossover even at lower temperatures. Both curves exhibit maximum values in the vicinity of T_c.

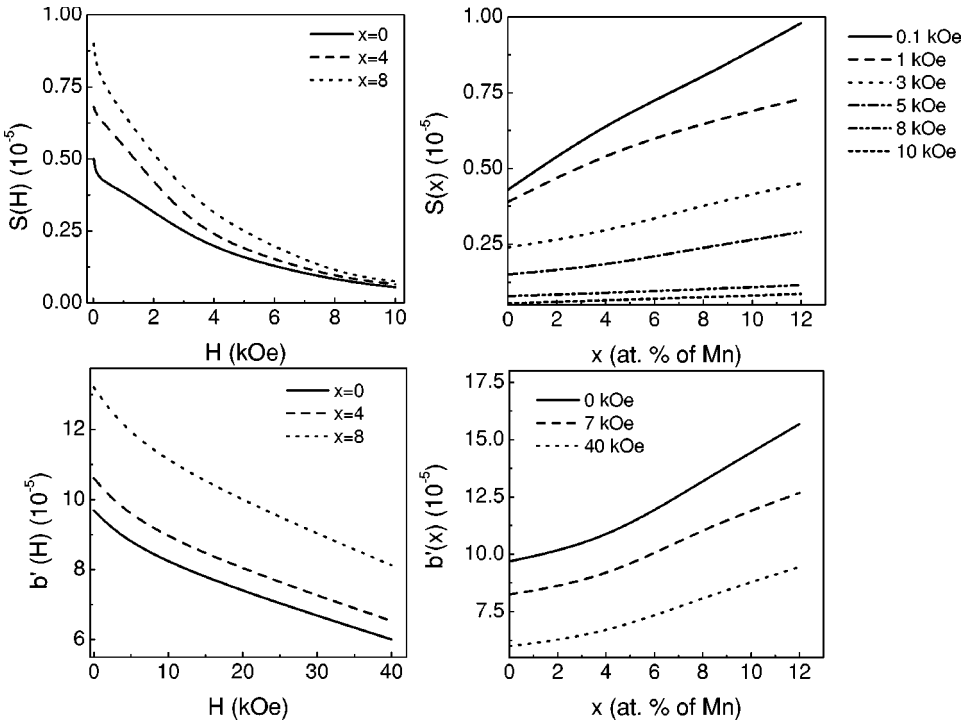

FIG. 4. The dependence of spin-fluctuation term S (Refs. 10 and 32) and the coefficient b' [Eq. (2)] on the applied magnetic field and concentration of Mn for amorphous $Fe_{90-x}Mn_xZr_{10}$ alloys.

(ii) As the Mn concentration increases, $\Delta\rho/\rho$ tends to be more positive below T_c.

(iii) On close observation, the MR (at 40 kOe) shows a steeper rise at low temperature and a broad maximum can be seen in the case of $x=8$ sample.

(iv) In all the cases $\Delta\rho/\rho$ decreases above the Curie temperature.

These results are quite consistent with the field-dependent data. A small hump observed at lower temperature and the existence of a maximum in MR close to T_c for various Mn concentration samples suggest that there is a close correlation between the magnetic and transport properties. The temperature dependence of MR may be explained as follows:

(i) Below T_c and above technical saturation, the MR is primarily due to the scattering of electrons from spin-wave excitations, which is found to decrease with increasing Mn concentration.[11] As a result of a reduction in electron-magnon scattering with temperature, this contribution to the MR decreases.

(ii) The reduction in the MR at temperatures below 50 K is much more rapid and for $x=8$ a broad hump could be seen. The observed hump in MR is well below the T_{sg} value of that particular composition.

The SG transition temperature occurs due to the lower level of frustration of spin systems, i.e., the increase of AFM coupling sites. It is well known that Mn couples antiferromagnetically to Fe. As the Mn concentration increases, it causes more frustration which would, in turn, lead to an increase in T_{sg}. Similarly, this phenomenon can be attributed to various models including the homogeneous exchange frustration model,[34] the FM-AFM cluster model,[35] the FM-FM cluster model,[36] and the transverse spin-freezing model.[37] However, recent Mössbauer studies indicate the development of a low-field peak in the hyperfine field distribution with Mn concentration, attributed to an increase in AFM coupling.[8] This phenomenon, obviously, makes it difficult to interpret the observed results by the homogeneous exchange frustration model,[34] where the decrease of the magnetic ordering temperature (T_c) is mainly attributed to a reduction in the FM interaction strength. Therefore, we deem that in field muon spin relaxation and Mössbauer measurements would shed some light on the microscopic spin structure of the present system and identify the model that could best explain the presently observed results.

Senoussi[38] has derived a linear dependence of MR versus H based on the quadratic dependence of MR on magnetization. According to Balberg,[39] the field dependence of MR at high fields is given by $(\Delta\rho/\rho)\propto H^{(1-\alpha)/(\beta\delta)}$ provided $\mu H/KT \gg |(1-T/T_c)|$, where μ is the magnetic moment of the ion and α, β, and δ are the traditional critical exponents. The experimental data on $Ni_{79}Mn_{21}$ of Senoussi,[38] however, do not show the claimed behavior since the exponent $m[(1-\alpha)/(\beta\delta)=0.63]$ is clearly less than unity. Our MR data near the critical region (above and below) have been fitted to the above equation (Fig. 8) and result in the exponent values $m=0.56$ (0.71) below (above) the critical temperature. These critical exponents are in close agreement with the magnetization data[40] and the exponents predicted for the 3D Heisenberg ferromagnet ($\alpha=-0.115$, $\beta=0.3645$, and $\delta=4.8$ yield $m=0.63$).

3. Composition dependence

The composition variation of the TMR for a-$Fe_{90-x}Mn_xZr_{10}$ alloys is shown in Fig. 9. The MR is observed to increase (decrease) at lower temperatures (above T_c) with increasing Mn concentration. These results are similar to the composition dependence of the dc susceptibility and the local magnetic anisotropy.[11] Within the frame

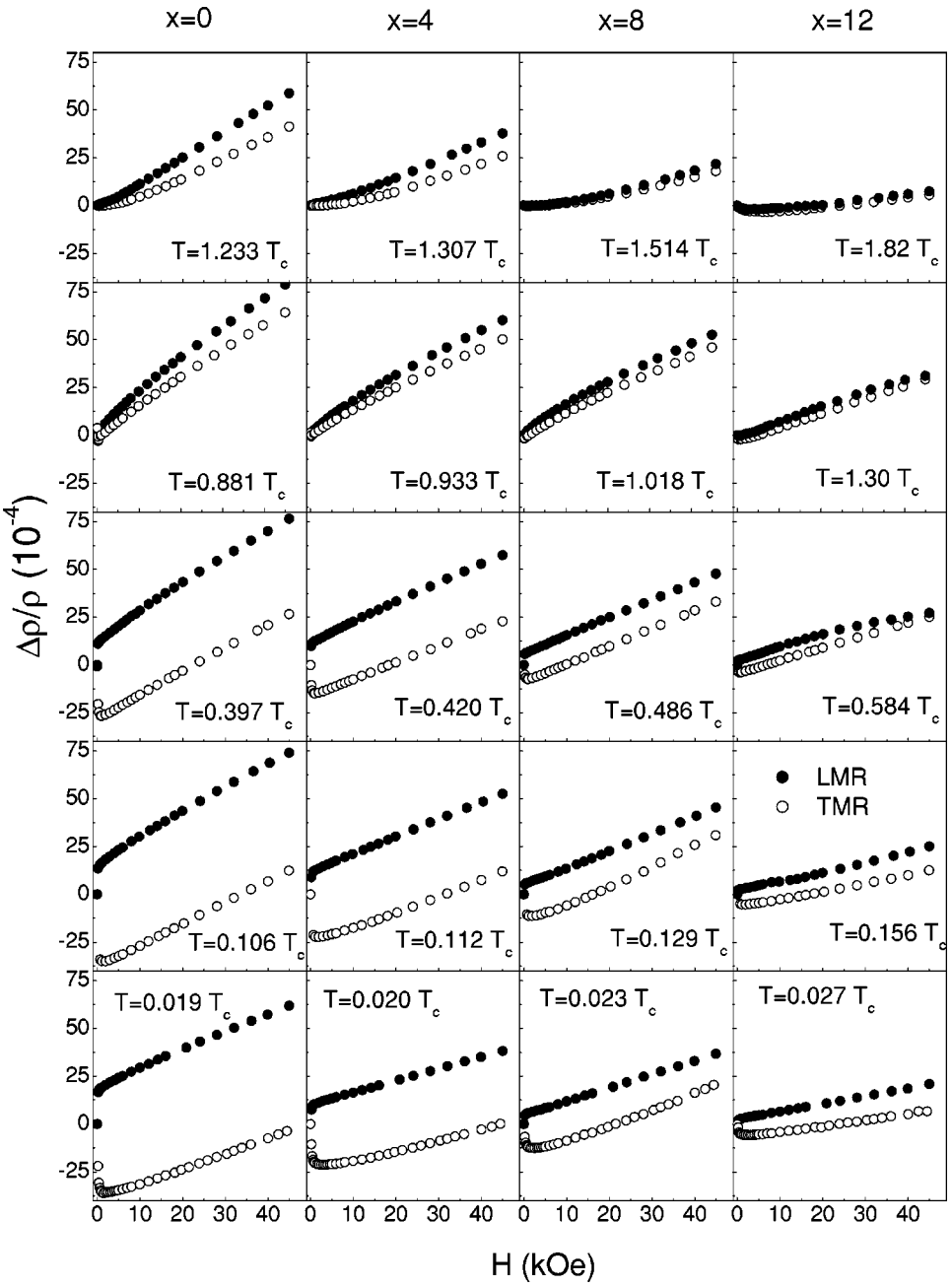

FIG. 5. Longitudinal (●) and transverse (o) magnetoresistance as a function of field for amorphous $Fe_{90-x}Mn_xZr_{10}$ alloys at different fixed temperatures.

work of the band model, the observed results can be understood as follows: The effect of increasing the Mn concentration should decrease the exchange splitting of the spin-up and spin-down *d* subbands and shift the Fermi level (E_F) to lower energies. This implies that E_F lies within the $d_\downarrow$ and $d_\uparrow$ subbands for the entire composition range of the present study. According to the itinerant model, the applied external field increases the splitting between the spin-up and spin-down subbands and hence, by analogy to the influence of increasing ΔE with an applied field, the MR decreases below the magnetic ordering temperature. Calculations of the magnetoresistivity of antiferromagnets using the molecular-field approximation[41] have shown that the MR is positive for the AFM state and negative for the FM state. In general, the suppression of spin-flip scattering by an external field gives rise to a negative contribution to the MR, and coherent spin scattering from different sites gives an additional contribution to the MR that may be either positive or negative. In the PM and FM states the magnetic field increases the effective field acting on the localized spins and suppresses the spin fluctuations, leading to a negative MR. On the other hand, in the AFM state the applied field may suppress the spin fluctuations on one site while increasing them on another site and the total MR, which is sum of the contributions from the two sites, may be positive. It is known that *a*-FeMnZr alloys possess mixed magnetic interactions and the resulting MR will be the sum of contributions from the various magnetic states. The magnetization curves of the present series of samples show that magnetic saturation is not obtained even up to a 6-T applied field.[4,11] The presence of both FM and AFM interactions leads to a frustration and guides the system into a noncollinear spin state at low temperature.

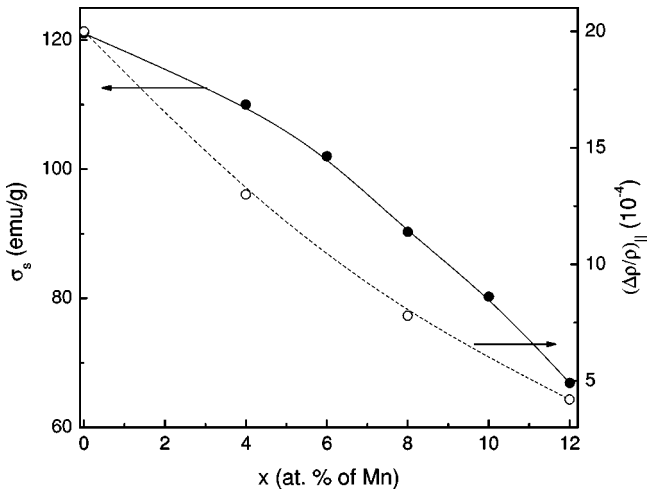

FIG. 6. The composition dependence of spontaneous magnetization and spontaneous magnetoresistance in longitudinal geometry for amorphous $Fe_{90-x}Mn_xZr_{10}$ alloys.

Finally, a comparison of the temperature dependence of magnetic and electrical transport characteristics are presented in Fig. 10. The temperature dependence of the static (field cooled and zero-field cooled) magnetization, ACS, $r(T)$, and MR are shown. The FM transition at $T_c = 180$ K is marked by a sudden increase in the real component of the ACS. At lower temperatures the ACS decreases, indicating a decrease in the relative importance of FM interactions. Near T_c, the resistivity exhibits a minimum, which is reflected quite well in the temperature derivative of resistivity (Fig. 1(b)). The low-temperature resistivity minimum in the higher Mn sample again corresponds to the maximum observed in the imaginary part of the ACS and this occurs close to the SG freezing temperature. The features observed in the MR near specific temperatures are reflected in the behavior of the ACS as well. This fact demonstrates that the MR as a function of temperature can also be used for characterizing the transitions in weak itinerant magnetic materials. It is indeed predicted from the spin-correlation model that the MR should have a strong temperature dependence centered around the magnetic transitions and the measured MR in the present work is consistent with this picture.

C. Spontaneous resistive anisotropy

The spontaneous resistive anisotropy (SRA) measures the difference in the resistivity of a single-domain ferromagnetic metal in zero induction, when the magnetization is parallel or perpendicular to the current direction, as shown by

$$\left(\frac{\Delta\rho}{\rho_0}\right)_s = \left(\frac{\rho_{||s} - \rho_{\perp s}}{\rho_0}\right). \tag{4}$$

It is important to comment on the procedure used to obtain the SRA as a function of temperature and composition. There has been earlier discussion[42] on whether the extrapolation from a magnetically saturated regime, necessary to determine the SRA from Eq. (4), should be based on applied field (H), the internal field [$\mu_0 H_i$; where $H_i = H - NM/(4\pi)$], or simply ignored owing to its inherent errors. We have adopted the extrapolation procedure down to $H = 0$ mainly due to the

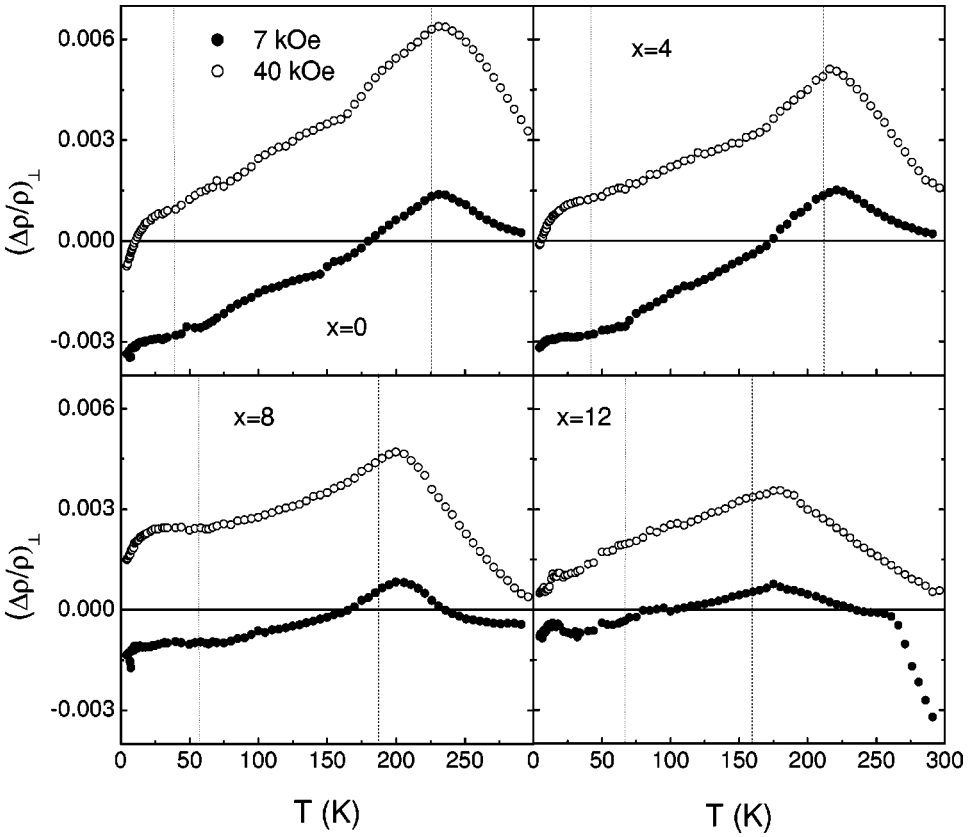

FIG. 7. Transverse magnetoresistance as a function of temperature at different fixed fields for amorphous $Fe_{90-x}Mn_xZr_{10}$ alloys.

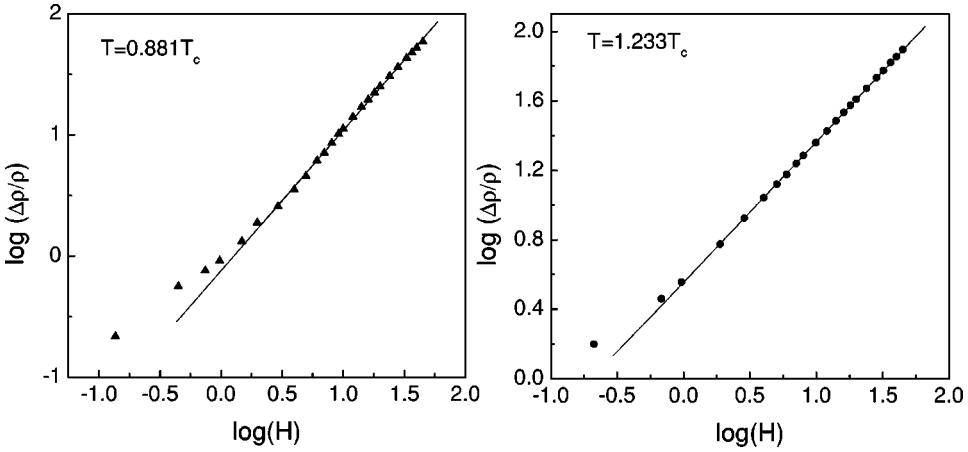

FIG. 8. Field dependence of magnetoresistance (plotted on a logarithmic scale) for the amorphous $Fe_{90}Zr_{10}$ alloy below and above the Curie temperature. The line passing through the data points is the best fit to $(\Delta\rho/\rho) \propto H^{(1-\alpha)/(\beta\delta)}$.

reason that for the Mn-doped FeZr and FeZr samples extrapolation from a magnetically saturated state is not possible since the saturation[11,37] is achieved only in applied fields of more than 6 T, far in excess of those available in the present experiment. As shown in Fig. 5, the MR shows a weak positive dependence on field for both orientations above the Curie temperature and this weak dependence decreases as the Mn concentration increases. Above 10 kOe, the MR increases almost linearly with field and the slope of the straight-line region decreases substantially with increasing Mn concentration. Moreover, we have not observed any nonzero SRA above the Curie temperature. This is expected since the system is far from its FM state and the applied field is not adequate to induce any appreciable changes in the polarization of spins at this temperature. By contrast, a nonzero SRA is observed below the Curie temperature. The technical saturation for the LMR is achieved at lower-field values than that for the transverse case. Moreover, the SRA is observed to decrease not only with increasing Mn concentration, but also with temperature for a particular concentration. The physical parameters obtained from Fig. 5 are listed in Table III and also depicted in Fig. 11(a). According to the two-current-conduction model, the spin-up and spin-down electrons conduct in parallel and the SRA is a consequence of the anisotropic $d_\uparrow$-$d_\downarrow$ mixing caused by the spin-orbit interaction.[43] Calculations based on this model yield the following expressions for the SRA:[44]

$$\left(\frac{\Delta\rho_s}{\rho_0}\right) = \gamma'\left(\frac{\rho_\downarrow^0 - \rho_\uparrow^0}{\rho_\uparrow^0}\right) + 3\beta\frac{\rho_\downarrow^0}{\rho_\downarrow^0 + \rho_\uparrow^0}, \tag{5}$$

where $\beta = -0.08(\lambda'/\Delta)^2(1-4\cos^2\eta_2^\uparrow)\sin^2\eta_2^\uparrow$, λ' is the local spin-orbit coupling constant, Δ is the virtual bound-state width, and $\rho_\uparrow^0$, $\rho_\downarrow^0$ are the residual resistivity for spin-up and spin-down electrons, respectively. The value of γ' is estimated to be 0.01 from a large amount of experimental data on the SRA of Fe- and Ni-based alloys. For the $3d$ transition metals, $\lambda' \ll \Delta$ and hence the second term in Eq. (5) can be safely neglected for the present alloys, i.e., Eq. (5) becomes

$$\left(\frac{\Delta\rho_s}{\rho_0}\right) = \gamma'\left(\frac{\rho_\downarrow^0 - \rho_\uparrow^0}{\rho_\uparrow^0}\right). \tag{6}$$

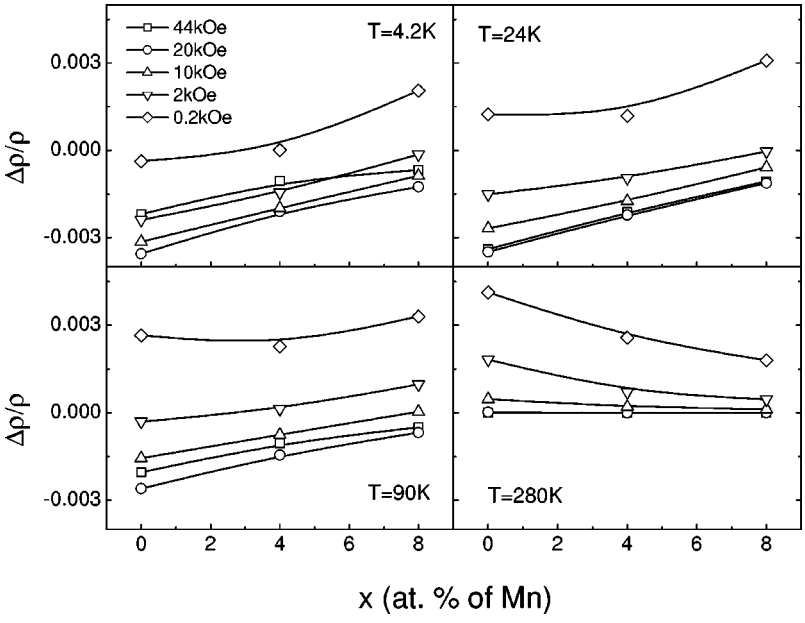

FIG. 9. Composition dependence of the transverse magnetoresistance plotted at different temperatures and fields for amorphous $Fe_{90-x}Mn_xZr_{10}$ alloys.

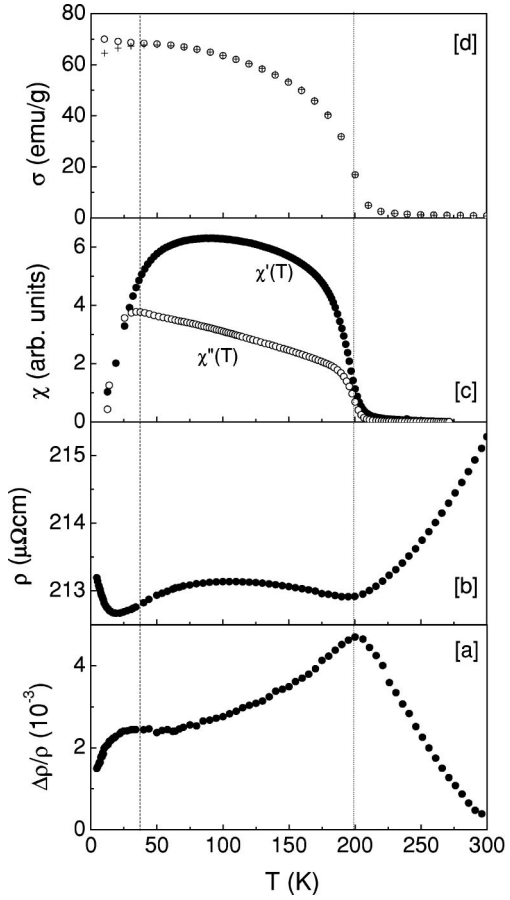

FIG. 10. (a) Magnetoresistance, (b) resistivity, (c) real (χ'), and imaginary (χ'') components of ac susceptibility and (d) magnetization [field-cooled (o) and zero-field-cooled (+) curves] as a function of temperature for the amorphous $Fe_{82}Mn_8Zr_{10}$ alloy.

This provides a criterion for determining whether a given alloy is a strong or a weak ferromagnet (a strong ferromagnet has holes only in the $d_\downarrow$ band while a weak ferromagnet has holes and electrons in both $d_\uparrow$ and $d_\downarrow$ bands) as follows: $\rho_\downarrow^0$ and $\rho_\uparrow^0$ possess comparable values for a weak ferromagnet since vacant states are available in both $d_\uparrow$ and $d_\downarrow$ for s electrons to make transitions, whereas the values of $\rho_\downarrow^0$ greatly exceed that of $\rho_\uparrow^0$ in a strong ferromagnet because s-d scattering is allowed only for spin-down electrons since there are no vacant $d_\uparrow$ states at the Fermi level.

In order to obtain information about the electronic structure, the contributions of spin-up and spin-down electrons to the resistivity are calculated with the help of the following expressions:

$$\rho_\downarrow^0(x)=\rho_0(x)\left[\frac{1}{\gamma'}\frac{\Delta\rho_s(x)}{\rho_0}+2\right], \tag{7}$$

$$\rho_\uparrow^0(x)=\rho_\downarrow^0(x)\left[\frac{1}{\gamma'}\frac{\Delta\rho_s(x)}{\rho_0}+1\right]^{-1}, \tag{8}$$

where ρ_0 is the residual resistivity. The composition dependence of the SRA obtained at different temperatures is used to calculate the subband contribution to the resistivity as given in Eqs. (7) and (8) and the determined values are plotted as a function of composition at 4.2 K in Fig. 11(b). The observation of decreasing SRA with increasing temperature can be understood in the following general terms: As the temperature is increased, thermal fluctuations compete with the exchange splitting, leading to equalization in the subband occupations, i.e., the difference between the two terms in the numerator of Eq. (6) decreases. This process evolves continuously until T_c is reached, at which point the static exchange splitting collapses and the SRA vanishes. The decrease of the SRA with increasing Mn concentration indicates that the exchange splitting decreases as the Mn concentration increases. The SRA and high-field susceptibility calculated at 4.2 K is plotted as a function of Mn concentration in Fig. 12(a). The large value of the high-field susceptibility, caused by the flipping of weakly coupled AFM spins in high field, is a characteristic feature of the Invar effect. From the above discussion, it is tempting to suggest the possible existence of a noncollinear spin structure in the present series. Particularly, below T_c, the variation of the high-field susceptibility for all samples shows behavior that is typical for weak itinerant[11,45] ferromagnets. Finally, we focus our attention on the relation between the SRA and magnetization, defined as $(\Delta\rho/\rho_0)_s=z\sigma^n$, where σ is the magnetization, and z and n are constants. The value of σ is taken from the magnetization data. Figure 12(b) shows the relation between the SRA and magnetization for a-$Fe_{86}Mn_4Zr_{10}$ alloys at different temperatures. The value of n increases from 2 in the intermediate-temperature range and has a peak value of ap-

TABLE III. Estimation of spontaneous resistive anisotropy (SRA) from extrapolation technique ("p") and technical saturation ("q") for amorphous $Fe_{90-x}Mn_xZr_{10}$ ($x=0$, 4, 8, and 12) alloys at different temperatures. All the entries for SRA must be multiplied by 10^{-4}.

x	4.2 K		24 K		90 K		200 K		280 K	
	p	q	p	q	p	q	p	q	p	q
0	59.3	58.56	55.81	56.23	42.34	41.01	5.52	5.33	3.36	3.16
4	35.1	34.24	38.58	36.95	28.87	26.79	2.90	2.84	1.26	1.25
8	21.8	21.25	21.02	19.98	15.33	14.68	1.45	1.23	0.33	0.21
12	08.4	08.13	07.05	06.78	06.54	06.63	0.55	0.42	0.02	0.08

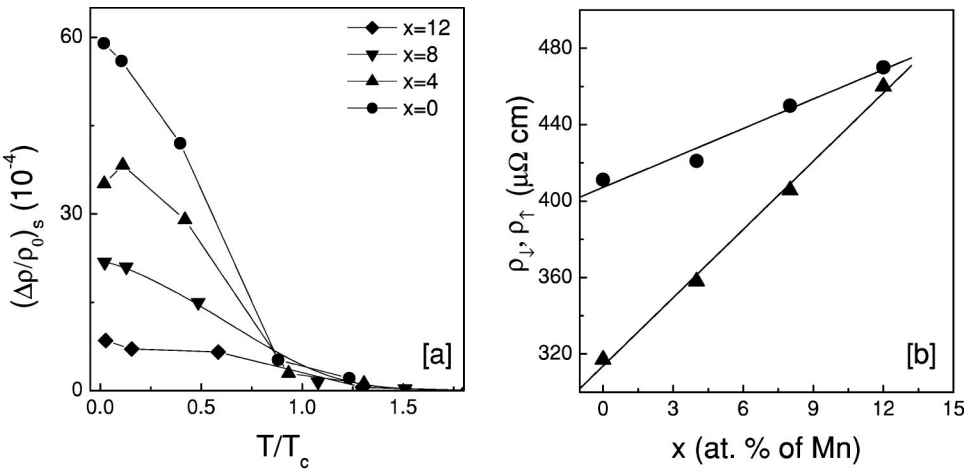

FIG. 11. (a) The spontaneous resistive anisotropy as a function of reduced temperature with respect to Curie temperature for different Mn concentrations. (b) The spin-up and spin-down contributions to the total resistivity determined from the two-current-conduction model.

proximately ($n=$) 5 at $T=T_c$. One may understand this behavior by considering that as T_c is approached from either above or below, the effect of the magnetic field on transport properties such as resistivity that are dominated by the short-range order would be different than those such as magnetization that are determined by long-range behavior.

IV. CONCLUSIONS

Electrical transport, magnetotransport, and magnetization studies of amorphous $Fe_{90-x}Mn_xZr_{10}$ alloys have been carried out in the temperature region of 4.2 K to 300 K. The electrical resistivity of all alloys shows a minimum close to the Curie temperature and the higher Mn content alloys show a second minimum at lower temperature. Diffusion associated with longitudinal spin fluctuations of the magnetization is responsible for the electrical resistivity at low temperatures, while the electron-electron interaction effects account for the resistivity behavior in the temperature range 10 to 30 K. Detailed analysis of resistivity data indicates enhancement (suppression) of spin-density fluctuations with Mn concentration (magnetic field). These results indicate that magnetic ordering has a considerable influence on both the resistivity and magnetoresistivity. This shows that the magnetoresistivity can be used to identify reentrant spin-glass behavior in these random ferromagnets. The resistive anisotropy measurements show that the SRA first appears at a temperature very close to the FM ordering temperature and confirms the emergence of an exchange field at that temperature. The observed SRA is explained on the basis of the two-current-conduction model. The high-field susceptibility data obtained from the magnetization measurements indicate that the alloys investigated in the present work are weak itinerant ferromagnets.

ACKNOWLEDGMENTS

The authors would like to thank the Council of Scientific and Industrial Research (CSIR), New Delhi, India, for providing financial support for this work. Work conducted at Dalhousie University has been funded by the Natural Sciences and Engineering Research Council of Canada and the Killam Fund.

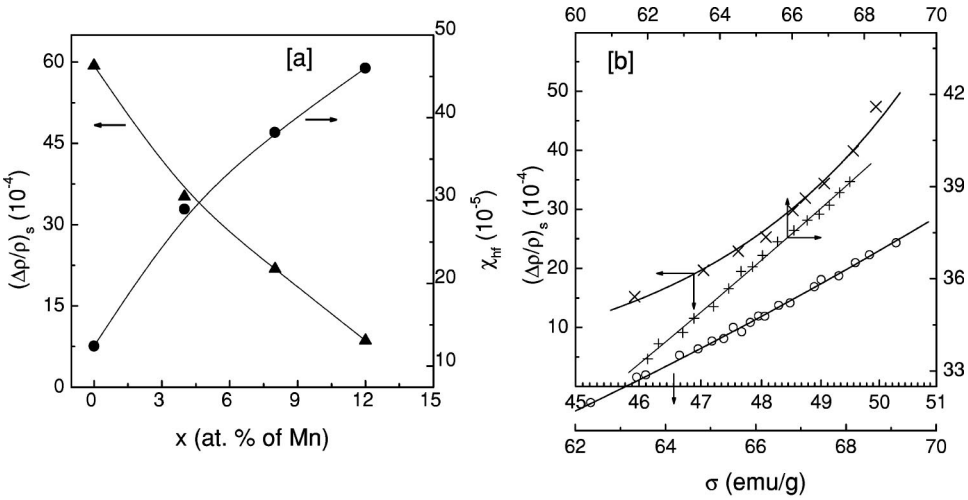

FIG. 12. (a) The SRA and high-field susceptibility as a function of Mn concentration at 4.2 K for a-$Fe_{90-x}Mn_xZr_{10}$ alloys, (b) the relation between SRA and magnetization at different temperatures 4.2 K ($n=1.809$), 100 K ($n=2.242$), and 200 K ($n=5.204$) for the a-$Fe_{86}Mn_4Zr_{10}$ alloy.

*Electronic address: veeturi@phy.iitkgp.ernet.in
†Present address: Department of Physics and Center for Nanospinics of Spintronic Materials, Korea Advanced Institute of Science and Technology (KAIST), Taejeon 305 701, South Korea.

[1] D. Stauffer and A. Aharony, *Introduction to Percolation Theory* (Taylor & Francis, London, 1991); A.G. Bernat, X. Chen, H.P. Kunkel, and G. Williams, Phys. Rev. B **52**, 10 160 (1995).
[2] K. Balakrishnan and S.N. Kaul, Phys. Rev. B **65**, 134412 (2002); S.N. Kaul and S. Srinath, *ibid.* **63**, 94410 (2001); M. Dudka, R. Folk, Yu. Holovatch, and D. Ivaneiko, J. Magn. Magn. Mater. **256**, 243 (2003).
[3] K. Shirakawa, K. Fukamichi, T. Kaneko, and T. Masumoto, Sci. Rep. Res. Inst. Tohoku Univ. A **31**, 54 (1983).
[4] B.G. Shen, R. Xu, J. Zhao, and W. Zhan, Phys. Rev. B **43**, 11 005 (1991).
[5] L.F. Barquin, J.C. Gomez Sal, P.D. Babu, and S.N. Kaul, J. Magn. Magn. Mater. **133**, 82 (1994).
[6] V. Srinivas, A.K. Nigam, G. Chandra, D.W. Lawther, M. Yewondwossen, and R.A. Dunlap, J. Appl. Phys. **76**, 6501 (1994).
[7] D.G. Plaza, L.F. Barquin, J.G. Soldevilla, R. Antras, and J.C. Gomez Sal, Solid State Commun. **102**, 353 (1997).
[8] P.L. Paulose, S. Bhattacharya, V. Nagarajan, and R. Nagarajan, Solid State Commun. **104**, 767 (1997).
[9] V. Srinivas, Phys. Status Solidi B **207**, 233 (1998); Proc. Mater. Sci. Soc. India **1**, SC 65 (1995).
[10] A. Perumal, K.S. Kim, V. Srinivas, S.C. Yu, V.V. Rao, and R.A. Dunlap, J. Magn. Magn. Mater. **226-230**, 1329 (2001); A. Perumal, V. Srinivas, V.V. Rao, and R.A. Dunlap, Physica B **292**, 164 (2000).
[11] A. Perumal, V. Srinivas, K.S. Kim, S.C. Yu, V.V. Rao, and R.A. Dunlap, Phys. Rev. B **65**, 64428 (2002).
[12] S. Kirkpatrick and D. Sherrington, Phys. Rev. B **17**, 4384 (1978); M. Gabay and G. Toulouse, Phys. Rev. Lett. **47**, 201 (1981); J.R. Thomson, H. Guo, D.H. Ryan, M.L. Zuckermann, and M. Grant, Phys. Rev. B **45**, 3129 (1992).
[13] P. Pureur, W.H. Schreiner, J.V. Kunzler, D.H. Ryan, and J.M.D. Coey, Solid State Commun. **65**, 163 (1988).
[14] S.N. Kaul, W. Kettler, and M. Rosenberg, Phys. Rev. B **35**, 7153 (1987).
[15] P.D. Babu, S.N. Kaul, L.F. Barquin, and J.C. Gomez Sal, J. Magn. Magn. Mater. **140-144**, 295 (1995).
[16] G. Bergmann, Phys. Rep. **107**, 1 (1984); G. Bergmann, Phys. Rev. Lett. **57**, 1460 (1986).
[17] L.F. Barquin, J.C. Gomez Sal, R. Hauser, and E. Bauer, J. Magn. Magn. Mater. **196-197**, 148 (1999).
[18] K. Suzuki, J.W. Cochrane, A. Aoki, and J.M. Cadogan, J. Magn. Magn. Mater. **242-245**, 273 (2002).
[19] H. Yamauchi, H. Onodera, and H. Yamamoto, J. Phys. Soc. Jpn. **53**, 747 (1984).
[20] H. Yamamoto, H. Onodora, K. Hosoyama, T. Masumoto, and H. Yamauchi, J. Magn. Magn. Mater. **31-34**, 1579 (1983); I. Abu-Aliarayesh and M.R. Said, *ibid.* **210**, 73 (2000); G.D. Mukherjee, S. Chakraborty, D.D. Rathnayaka, D.G. Naugle, and A.K. Majumdar, *ibid.* **214**, 185 (2000).
[21] A. Perumal, Ph.D thesis, Indian Institute of Technology, Kharagpur, 2002.
[22] G.A. Takzey, I.I. Sych, and A.Z. Menshikov, Fiz. Met. Metalloved. **52**, 1157 (1981).
[23] J. Kastner and D.M. Herlach, J. Magn. Magn. Mater. **51**, 305 (1985); B.E. Babic, Z. Marohnic, M. Ocko, A. Hamzic, K. Saub, and B. Pivac, *ibid.* **15-18**, 934 (1980); A. Fert and R. Asomoza, J. Appl. Phys. **50**, 1886 (1979).
[24] A. Perumal, V. Srinivas, V.V. Rao, and R.A. Dunlap, Indian J. Pure Appl. Phys. **38**, 35 (2000).
[25] J. Kondo, Prog. Theor. Phys. **27**, 772 (1962); J. Kondo, *Solid State Physics*, edited by F. Seitz, D. Turnbull, and H. Ehernreich (Academic, New York, 1969), Vol. 23, p. 184.
[26] D. Dahlberg, K.V. Rao, and K. Fukamichi, J. Appl. Phys. **55**, 1942 (1984).
[27] B.L. Altshuler and A.G. Aronov, Sov. Phys. JETP **50**, 968 (1968).
[28] K.V. Rao, *Amorphous Metallic Alloys*, edited by F.E. Luborsky (Butterworth, London, 1983), p. 426.
[29] K. Ueda and T. Moriya, J. Phys. Soc. Jpn. **39**, 605 (1975).
[30] T. Moriya and A. Kawabata, J. Phys. Soc. Jpn. **34**, 639 (1973); **35**, 669 (1975).
[31] S. Chakravarty and A. Schmid, Phys. Rep. **140**, 193 (1986).
[32] The spin-fluctuation term S is defined as $m(H) = [M(H,T)/M(0,T)] = 1 - S(H)T^2$. More details may be found in Ref. 10.
[33] D. Kaptas, T. Kemeny, L.F. Kiss, J. Balogh, L. Granasy, and I. Vincze, Phys. Rev. B **46**, 6600 (1992).
[34] H. Ren and D.H. Ryan, Phys. Rev. B **51**, 15 885 (1995).
[35] D.A. Read, T. Moyo, and G.C. Hallam, J. Magn. Magn. Mater. **44**, 279 (1984); D.A. Read, T. Mayo, S. Jassim, R.A. Dunlap, and G.C. Hallam, *ibid.* **82**, 87 (1989);
[36] S.N. Kaul, J. Magn. Magn. Mater. **53**, 5 (1986); S.N. Kaul, J. Phys.: Condens. Matter **3**, 4027 (1991); S.N. Kaul, V. Siruguri, and G. Chandra, Phys. Rev. B **45**, 12 343 (1992).
[37] D.H. Ryan, J.M.D. Coey, E. Batalla, Z. Altounian, and J.O. Strom-Olsen, Phys. Rev. B **35**, 8630 (1987); D.H. Ryan, in *Magnetic Properties of Amorphous Metals*, edited by A. Hernando, V. Madurga, M.C.S.- Trujillo, and M. Vazquez (Elsevier, Amsterdam, 1987), p. 244.
[38] S. Senoussi, J. Phys. F: Met. Phys. **10**, 2491 (1980).
[39] I. Balberg, Physica B **91**, 71 (1977).
[40] A. Perumal, V. Srinivas, K.S. Kim, S.C. Yu, V.V. Rao, and R.A. Dunlap, J. Magn. Magn. Mater. **233**, 280 (2001).
[41] H. Yamada and S. Takada, J. Phys. Soc. Jpn. **34**, 51 (1973).
[42] Y. Hsu, S. Jen, and L. Berger, J. Appl. Phys. **50**, 1907 (1979).
[43] A.P. Malozemoff, Phys. Rev. B **32**, 6080 (1985); **34**, 1853 (1986).
[44] O. Jaoul, I.A. Campbell, and A. Fert, J. Magn. Magn. Mater. **5**, 23 (1977).
[45] A. Perumal and V. Srinivas, Phys. Rev. B **67**, 094418 (2003).